

# Exchange Interactions at the Supramolecular Level – Synthesis, Crystal Structure, Magnetic Properties, and EPR Spectra of $[\text{Mn}(\text{MAC})(\text{TCNQ})_2]$ (MAC = Pentaaza Macrocyclic Ligand; $\text{TCNQ}^{\cdot-}$ = Radical Anion of 7,7,8,8-Tetracyano-*p*-quinodimethane)

Augustin M. Madalan,<sup>[a,b]</sup> Violeta Voronkova,<sup>[c]</sup> Ravil Galeev,<sup>[c]</sup> Ludmila Korobchenko,<sup>[c]</sup> Jörg Magull,<sup>[a]</sup> Herbert W. Roesky,<sup>\*[a]</sup> and Marius Andruh<sup>\*[b]</sup>

*Dedicated to Professor Achim Müller on the occasion of his 65th anniversary*

**Keywords:** Manganese / N ligands / Stacking interactions / Magnetic properties / EPR spectroscopy / Radicals

The reaction between  $[\text{Mn}(\text{MAC})(\text{H}_2\text{O})_2]\text{Cl}_2 \cdot 4\text{H}_2\text{O}$  and  $\text{LiTCNQ}$  (MAC = 2,13-dimethyl-3,6,9,12,18-pentaazabicyclo[12.3.1]octadeca-1(18),2,12,14,16-pentaene) affords a complex with the formula  $[\text{Mn}(\text{MAC})(\text{TCNQ})_2]$  (**1**), whose crystal structure has been determined. Its structure consists of neutral mononuclear entities. The manganese(II) ion is heptacoordinated, with a pentagonal bipyramidal geometry. The apical positions are occupied by the  $\text{TCNQ}^{\cdot-}$  radicals, while the macrocyclic ligand is coordinated at the equatorial positions. The seven Mn–N distances range from 2.273(3) to 2.301(6) Å. The strong intermolecular  $\pi$ – $\pi$  stacking interactions between the TCNQ radicals (3.2 Å) leads to weave-like

infinite chains, which propagate along the crystallographic *c* axis. The cryomagnetic investigation of **1** revealed a weak intermolecular antiferromagnetic coupling of the  $\text{Mn}^{2+}$  ions ( $J = -0.18 \text{ cm}^{-1}$ ), which is mediated by the diamagnetic  $(\text{TCNQ})_2^{2-}$  pairs resulting from the stacking interactions in the crystal. The intermolecular exchange interaction between the  $\text{Mn}^{2+}$  ions was further confirmed by variable temperature EPR spectroscopic measurements [ $|J| = 0.15(5) \text{ cm}^{-1}$ ], which have been carried out in both the X and Q bands.

(© Wiley-VCH Verlag GmbH & Co. KGaA, 69451 Weinheim, Germany, 2003)

## Introduction

Since the pioneering work of Melby et al.,<sup>[1]</sup> the  $\text{TCNQ}^{\cdot-}$  radical has been widely used as a building-block for the construction of molecular solids with exciting physical properties.<sup>[2]</sup> Among these the magnetic ordering,<sup>[3]</sup> as well as the electrical conductivity are particularly attractive.<sup>[4]</sup> The neutral TCNQ molecule acts as a strong acceptor due to its low reduction potential to form the radical anion,  $\text{TCNQ}^{\cdot-}$ . The reaction between various metallocenes,  $[\text{M}(\text{Cp}^*)_2]$  ( $\text{Cp}^* = \text{C}_5\text{Me}_5$ ) with TCNQ leads to a family of charge transfer complexes,  $[\text{M}(\text{Cp}^*)_2]^+[\text{TCNQ}]^{\cdot-}$ , with strong magnetic interactions between the spin carriers. Some of these compounds are molecular magnets.<sup>[5]</sup>

Due to its high  $\sigma$ -donor character towards transition-metal ions, the  $\text{TCNQ}^{\cdot-}$  ion can act as a ligand generating a rich coordination chemistry.<sup>[6,7]</sup> The synthetic approach consists of the reaction of transition-metal complexes with  $\text{LiTCNQ}$ . The  $\text{TCNQ}^{\cdot-}$  radical coordinates at a vacant site on the metal centre, or replaces a weakly coordinated ligand in the coordination sphere of the metal ion. Most of these complexes have the general formula  $[\text{M}(\text{N}_4)(\text{TCNQ})_2]$ , where ( $\text{N}_4$ ) denotes various polyamine ligands (e.g. tetraazamacrocyclic ligands, open tetraamines, two ethylenediamine molecules, etc.) and  $\text{M}^{2+} = \text{Fe}^{2+}$ ,<sup>[8]</sup>  $\text{Ni}^{2+}$ ,<sup>[9]</sup>  $\text{Cu}^{2+}$ ,<sup>[10]</sup> and  $\text{Co}^{2+}$ .<sup>[10a]</sup> Using  $\text{TCNQ}^{\cdot-}$  as a ligand, we have recently synthesised the first coordination compound containing three different types of spin carriers: 2p ( $\text{TCNQ}^{\cdot-}$ ), 3d ( $\text{Cu}^{2+}$ ) and 4f ( $\text{Gd}^{3+}$ ).<sup>[11]</sup> The  $\text{TCNQ}^{\cdot-}$  species coordinates to both  $\text{Cu}^{2+}$  and  $\text{Gd}^{3+}$  ions.

As a part of our research program on the exchange interactions mediated by  $\pi$ – $\pi$  stacking, we report here the synthesis, crystal structure, magnetic and EPR spectroscopic properties of a new  $\text{Mn}^{2+}$ – $\text{TCNQ}^{\cdot-}$  compound,  $[\text{Mn}(\text{MAC})(\text{TCNQ})_2]$ , where MAC stands for the pentaazamacrocyclic ligand (2,13-dimethyl-3,6,9,12,18-pentaazabicyclo[12.3.1]octadeca-1(18),2,12,14,16-pentaene).

<sup>[a]</sup> Institut für Anorganische Chemie der Universität, Tammannstr. 4, 37077 Göttingen, Germany  
E-mail: hroesky@gwdg.de

<sup>[b]</sup> Inorganic Chemistry Laboratory, Faculty of Chemistry, University of Bucharest, Str. Dumbrava Rosie nr. 23, 70254 Bucharest, Romania  
E-mail: marius.andruh@dnt.ro

<sup>[c]</sup> Zawoisky Physical-Technical Institute of the Russian Academy of Sciences, Department of Chemical Physics, Laboratory of Molecular Photochemistry, Sibirsky Trakt 10/7, Kazan, Russia

## Results and Discussion

### Description of the Structure

The structure of compound **1** consists of mononuclear entities with the TCNQ<sup>•−</sup> anions coordinated to the metal ion (Figure 1). The manganese(II) ion exhibits a coordination number of seven with a pentagonal bipyramidal geometry. The TCNQ<sup>•−</sup> groups are coordinated in the apical positions, while the equatorial positions are occupied by the nitrogen atoms of the macrocyclic ligand. The seven Mn–N distances range from 2.273(3) to 2.301(6) Å. The shortest Mn–N distance corresponds to the Mn–pyridyl nitrogen bond. Selected bond lengths and angles are given in Table 1. The values of the interatomic distances in the TCNQ species are diagnostic of their electronic nature. In the case of compound **1**, the carbon–carbon distances fall in the range expected for TCNQ<sup>•−</sup> anions.<sup>[2,4c]</sup>

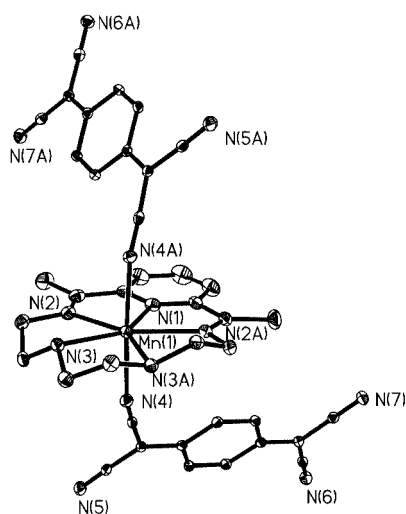
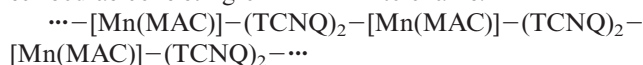


Figure 1. Molecular structure of [Mn(MAC)(TCNQ)<sub>2</sub>] and the atom numbering scheme.

Table 1. Selected bond lengths (Å) and angles (°) (symmetry codes i: 2 – x, y, 2.5 – z)

Mn1–N1	2.273(3)		
Mn1–N4 <sup>i</sup>	2.285(6)		
Mn1–N4	2.285(6)		
Mn1–N3	2.297(3)		
Mn1–N3 <sup>i</sup>	2.297(3)		
Mn1–N2 <sup>i</sup>	2.301(6)		
Mn1–N2	2.301(6)		
N1–Mn1–N4 <sup>i</sup>	86.21(6)	N1–Mn1–N4	86.21(6)
N4 <sup>i</sup> –Mn1–N4	172.42(8)	N1–Mn1–N3	142.27(6)
N4 <sup>i</sup> –Mn1–N3	91.17(8)	N4–Mn1–N3	94.82(8)
N1–Mn1–N3 <sup>i</sup>	142.27(6)	N4 <sup>i</sup> –Mn1–N3 <sup>i</sup>	94.82(8)
N4–Mn1–N3 <sup>i</sup>	91.17(8)	N3–Mn1–N3 <sup>i</sup>	75.46(8)
N1–Mn1–N2 <sup>i</sup>	69.47(6)	N4 <sup>i</sup> –Mn1–N2 <sup>i</sup>	87.01(8)
N4–Mn1–N2 <sup>i</sup>	90.34(8)	N3–Mn1–N2 <sup>i</sup>	148.05(8)
N3 <sup>i</sup> –Mn1–N2 <sup>i</sup>	72.92(8)	N1–Mn1–N2	69.47(6)
N4 <sup>i</sup> –Mn1–N2	90.34(8)	N4–Mn1–N2	87.01(8)
N3–Mn1–N2	72.92(8)	N3 <sup>i</sup> –Mn1–N	2148.05(8)
N2 <sup>i</sup> –Mn1–N2	138.94(8)		

An analysis of the packing diagram reveals interesting interactions at the supramolecular level. The small separations between anionic radicals arising from different [Mn(MAC)(TCNQ)<sub>2</sub>] units (3.2 Å) indicate the occurrence of strong  $\pi$ – $\pi$  interactions. Consequently, the overlap of the TCNQ<sup>•−</sup>  $\pi$  clouds generates weave-like chains propagating along the crystallographic *c* axis (Figure 2). The distance between the manganese atoms within the supramolecular chain is 13.03 Å. Consequently, the structure can be described as consisting of 1-D infinite chains:



in which the [Mn(MAC)] moieties are connected through dimerized TCNQ<sup>•−</sup> ligands.

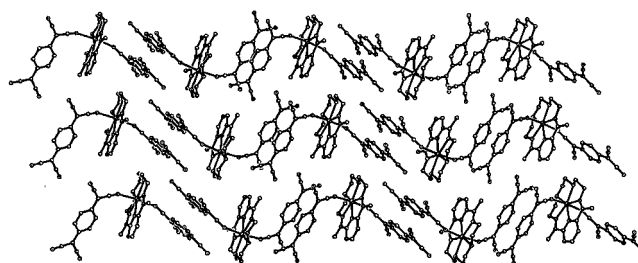


Figure 2. Packing diagram showing the formation of chains through the  $\pi$ – $\pi$  stacking interactions between the TCNQ radicals.

### Magnetic Measurements

The magnetic properties of compound **1** are shown in the form of an  $\chi_M T$  versus *T* plot (Figure 3). The value of the  $\chi_M T$  product at room temperature (4.2 cm<sup>3</sup> mol<sup>−1</sup> K) is lower than expected for the two types of spin carriers: Mn<sup>2+</sup> (*S* = 5/2) and two TCNQ<sup>•−</sup> radicals (each one with *S* = 1/2). In fact, the room temperature value corresponds exactly to *S* = 5/2, that is, only to one Mn<sup>2+</sup> (indeed, the expected value of the  $\chi_M T$  product for *S* = 5/2 is 4.37 cm<sup>3</sup> mol<sup>−1</sup> K). The lower value of the  $\chi_M T$  product at room temperature for **1** can be explained by the strong antiferromagnetic coupling between the stacked TCNQ<sup>•−</sup> radicals connecting the [Mn(MAC)]<sup>2+</sup> entities. This phenomenon has been observed with other compounds, where the stacking interactions between TCNQ<sup>•−</sup> radicals lead to diamagnetic (TCNQ)<sub>2</sub><sup>2−</sup> dimers.<sup>[2,9]</sup> As the temperature is lowered  $\chi_M T$  remains constant down to 70 K, then decreases abruptly, reaching a value of 1.9 cm<sup>3</sup> mol<sup>−1</sup> K at 2.0 K. Considering the TCNQ<sup>•−</sup> ions do not contribute to the magnetic moment of **1**, the magnetic properties can be simulated by taking into account only the [Mn(MAC)]<sup>2+</sup> units. The decrease of  $\chi_M T$  in the lower temperature range can be due to the zero-field splitting (*D*) of the manganese(II) ion and/or to a weak intermolecular antiferromagnetic interaction between the local spins mediated by the  $\pi$ – $\pi$  stacking interactions. A least-squares fit of the susceptibility data, taking into account the zero field splitting, led to *D* = 5.1 cm<sup>−1</sup>, a value which is too high for a manganese(II) complex. We recall that for the parent compound,

[Mn(MAC)(H<sub>2</sub>O)<sub>2</sub>]Cl<sub>2</sub>·4H<sub>2</sub>O, the value of the  $D$  parameter obtained from EPR spectroscopic measurements was found to be  $0.07\text{ cm}^{-1}$ .<sup>[12]</sup> The alternative way of rationalizing the magnetic behaviour is to consider only the exchange interactions of the manganese(II) ions within the supramolecular chain. The exchange pathway is provided by the diamagnetic (TCNQ)<sub>2</sub><sup>2-</sup> dimers. Consequently the magnetic data can be analysed using the Hamiltonian:  $\hat{H} = -J\sum S_i S_{i+1}$ . The temperature dependence of the magnetic susceptibility is given by Equation (1) and Equation (2):<sup>[14]</sup>

$$\chi_M^{\text{chain}} = \{Ng^2\beta^2 S_{\text{Mn}}(S_{\text{Mn}} + 1)/3kT\} \{(1+u)/(1-u)\} \quad (1)$$

(Fisher's infinite chain model) with:

$$u = \coth[JS_{\text{Mn}}(S_{\text{Mn}} + 1)/kT] - [kT/JS_{\text{Mn}}(S_{\text{Mn}} + 1)] \quad (2)$$

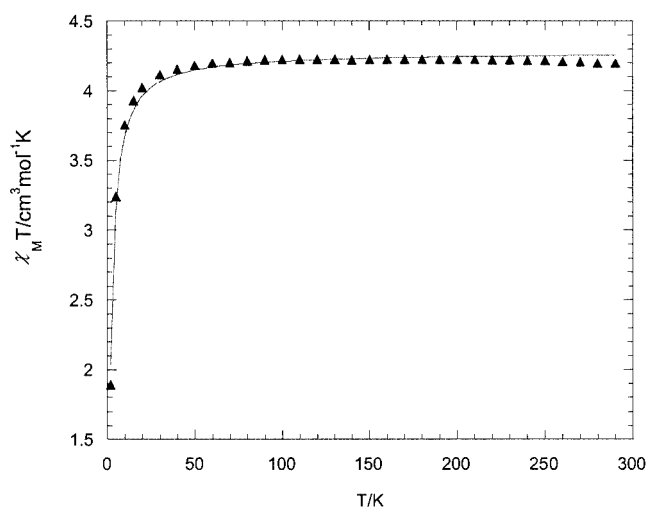


Figure 3. Temperature dependence of the  $\chi_M T$  product. The solid line represents the best fit curve.

The least-squares fit of the data leads to  $J = -0.18\text{ cm}^{-1}$  and  $g = 1.99$ . The low  $J$  value is quite reasonable, since the distance between the manganese(II) ions within a chain is large ( $13.03\text{ Å}$ ).

By fitting the data using the Curie–Weiss law,  $\chi_M^{-1} = (T - \theta)/C$ , we obtained  $\theta = -0.7\text{ K}$ ,  $C = 4.230\text{ cm}^3\text{mol}^{-1}\text{K}$  and  $g = 1.98$ . Given that  $\theta = zJ'S(S + 1)/3k$  and  $S = 5/2$ , it follows that  $zJ' = -0.34\text{ cm}^{-1}$ . As the packing diagram shows,  $z = 2$  and consequently  $J' = -0.17\text{ cm}^{-1}$ , in good agreement with Fisher's model.

### EPR Measurements

EPR spectra have been recorded on powder samples. Both X-band and Q-band (Figure 4) spectra consist of a single signal centred at  $g = 2.028(5)$ . The shape and the peak-to-peak linewidth of the signal,  $\Delta B$ , are frequency-dependent. A slight asymmetry of the signal with  $\Delta B = 945\text{ Oe}$  is observed in the X-band at room temperature, the shape

of the signal being intermediate between Lorentzian and Gaussian. As the frequency is increased, the asymmetry disappears and  $\Delta B$  decreases to  $595 \pm 50\text{ Oe}$  at room temperature (Figure 4). As the temperature is decreased, the linewidth of the signal increases. The measurements in the X-band show that this increase occurs mainly in the range of  $100\text{--}300\text{ K}$ , and at  $T = 12\text{ K}$   $\Delta B$  increases to  $1590 \pm 20\text{ Oe}$ . The temperature dependence of the spectrum in the Q-band shows that as the temperature is decreased, the linewidth increases from  $595 \pm 50\text{ Oe}$  at room temperature to  $1120 \pm 100\text{ Oe}$  at  $4.2\text{ K}$ .

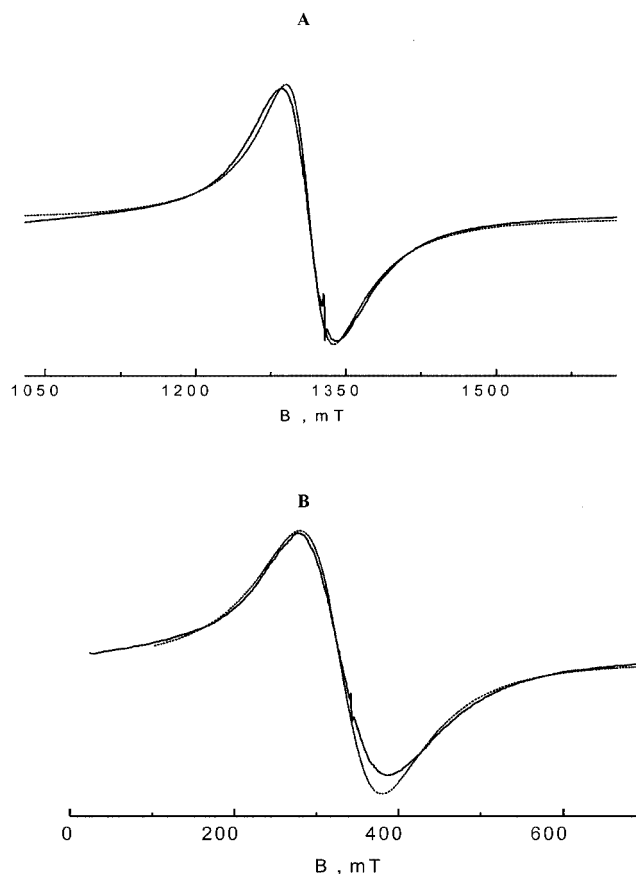


Figure 4. Experimental (solid lines) and simulated (dotted lines) EPR spectra at the Q-band (A) and at X-band (B) of compound **1** at room temperature. A narrow signal in the Q-band spectrum is due to the radical placed in the resonator for measuring the frequency.

The decrease in linewidth as a function of frequency is known as the "10/3" effect.<sup>[15]</sup> The frequency dependence of the linewidth of the signal has been previously observed for some compounds of  $\text{Mn}^{2+}$ .<sup>[16]</sup> This effect was interpreted using the Kuba and Tomita equation obtained for a simple cubic lattice composed of  $S = 1/2$  ions,<sup>[17]</sup> in which the frequency dependence of the linewidth of the signal is described as the frequency dependence of its dipole contribution. Our estimation of the dipole contribution to the linewidth of compound **1** shows that it is not determinant and cannot describe the frequency dependence observed for this compound.

The powder spectra of compound **1** do not show the fine and hyperfine structures due to the dipole–dipole and exchange interactions between neighbouring manganese(II) ions. It is known that if the exchange interaction,  $-JS_iS_{i+1}$ , exceeds the dipole-dipole and other interactions, an exchange-narrowed line is observed. The form of the EPR spectrum of the studied compound and its change with frequency and temperature were interpreted by supposing that the main contribution to the linewidth is due to the unresolved fine structure and not to the dipole–dipole interaction.

The frequency dependence of the EPR spectra was analysed using a simulation program that was written taking into account the fine structure [due to the zero-field splitting of manganese(II) ion] and the hyperfine structure for  $S = 5/2$ , the exchange interaction, and by averaging these structures according to the kinetic equations given in ref.<sup>[18]</sup> The linewidth of each component of the hyperfine structure was chosen by taking into account the dipole-dipole contribution. The value of the  $D$  parameter was taken as  $0.07 \text{ cm}^{-1}$ .<sup>[12]</sup> In the absence of the exchange interaction, the form of the spectrum of a polycrystalline  $\text{Mn}^{2+}$  sample in the X-band would be asymmetric. In the Q-band the form of the spectrum changes because the ratio between the fine structure parameter and the Zeeman energy changes. The exchange interaction averages out the fine structure but some differences in the X- and Q-bands remain. The observation of these differences enables us to estimate the  $J$  value. The asymmetry observed in the X-band is the manifestation of the incomplete averaging of the fine structure. The adjustment of the simulated and observed spectra at room temperature at the two frequencies allowed us to estimate the value of the exchange interaction  $|J|$  as  $0.15(5) \text{ cm}^{-1}$ , which is in reasonably good agreement with the value obtained through cryomagnetic measurements. In our model, the temperature dependence of the spectrum in the X-band can be explained by the change in either of the parameters  $D$  or  $J$ . The assumption about the change in the  $D$  parameter, which shows a certain change in the distortion of the nearest environment of  $\text{Mn}^{2+}$ , agrees with the EPR spectroscopic data of  $[\text{Mn}(\text{MAC})(\text{H}_2\text{O})_2]\text{Cl}_2 \cdot 4\text{H}_2\text{O}$ .<sup>[12]</sup> The increase of the linewidth in the Q-band, however, can be described only by a decrease in the  $J$  parameter. The EPR spectroscopic data therefore enable us to suppose that the exchange interaction decreases weakly as the temperature is decreased.

In conclusion, we have shown by means of two independent techniques (magnetic susceptibility and EPR spectroscopic measurements) that the intermolecular  $\pi$ – $\pi$  stacking of the  $\text{TCNQ}^{\cdot-}$  ligands, which leads to diamagnetic  $(\text{TCNQ})_2^{2-}$  dimers, is able to mediate weak exchange interactions between the manganese(II) ions.

## Experimental Section

**Preparation of  $[\text{Mn}(\text{MAC})(\text{TCNQ})_2]$  (**1**):** The manganese precursor,  $[\text{Mn}(\text{MAC})(\text{H}_2\text{O})_2]\text{Cl}_2 \cdot 4\text{H}_2\text{O}$ , was synthesised according to the lit-

erature.<sup>[12]</sup>  $\text{LiTCNQ}$  was obtained according to ref.<sup>[1]</sup> The reaction was carried out under oxygen-free nitrogen, using standard Schlenk techniques and degassed solvents. A solution of  $\text{LiTCNQ}$  (0.4 g, 1.9 mmol) in methanol/acetonitrile (1:1, 10 mL) was added dropwise to a solution of  $[\text{Mn}(\text{MAC})(\text{H}_2\text{O})_2]\text{Cl}_2 \cdot 4\text{H}_2\text{O}$  (0.44 g, 0.9 mmol) dissolved in methanol/acetonitrile (30 mL). The resultant mixture was allowed to stand at room temperature. After several hours, red crystals resulted, which were filtered off and washed with methanol/acetonitrile (1:1). IR data (KBr,  $\text{cm}^{-1}$ ):  $\tilde{\nu} = 3247 \text{ m}$ , 2188 vs, 2166 s, 1580 s, 1499 s, 1341 s, 1170 s, 1103 w, 937 w, 914 w, 818 m, 718 w, 476 w.  $\text{C}_{39}\text{H}_{29}\text{MnN}_{13}$  (734.68): calcd. C 63.76, H 3.98, N 24.78; found C 63.5, H 4.3, N 24.3.

**Crystallographic Data Collection and Structure Determination:** The diffraction intensities for compound **1** were collected on a STOE Image Plate IPDS II-System. The structures was solved by direct methods and refined against  $F^2$  by using SHELXL-97.<sup>[13]</sup> Heavy atoms were refined anisotropically. Hydrogen atoms were included using the riding model with  $U_{\text{iso}}$  tied to  $U_{\text{iso}}$  of the parent atoms. Crystallographic data and other pertinent information are summarised in Table 2. CCDC-196351 contains the supplementary crystallographic data for this paper. These data can be obtained free of charge at [www.ccdc.cam.ac.uk/conts/retrieving.html](http://www.ccdc.cam.ac.uk/conts/retrieving.html) [or from the Cambridge Crystallographic Data Centre, 12, Union Road, Cambridge CB2 1EZ, UK; Fax: (internat.) +44-1223/336-0033; E-mail: [deposit@ccdc.cam.ac.uk](mailto:deposit@ccdc.cam.ac.uk)].

Table 2. Crystal data and structure refinement for compound **1**

Empirical formula	$\text{C}_{39}\text{H}_{29}\text{MnN}_{13}$
Formula mass	734.68
Crystal system	monoclinic
Space group	$C2/c$
$a$ (Å)	10.6960(7)
$b$ (Å)	15.8054(13)
$c$ (Å)	21.2076(16)
$\beta$ (°)	93.93(1)
$V$ (Å <sup>3</sup> )	3576.81(15)
$Z$	4
$D_{\text{calcd.}}$ ( $\text{g cm}^{-3}$ )	1.364
$R_1$ [ $F_o > 4\sigma(F_o)$ ]	0.0478
$R_1$ (all data)	0.0546

**Other Measurements:** IR spectra (KBr pellets) were recorded on a BIO-RAD FTS 135 spectrometer. Magnetic susceptibility measurements were carried out using a SQUID magnetometer (MPMS Quantum Design). EPR measurements of the powder samples were carried out on ERS-230 and Varian spectrometers in the temperature range 300–10 K (X-band), 300–100 K and at 4.2 K (Q-band).

## Acknowledgments

A. M. M. and M. A. are grateful to the Alexander von Humboldt Foundation for financial support of this work. Support from the INTAS Program (Project 2000–00375) and the Deutsche Forschungsgemeinschaft is gratefully acknowledged. We thank Professor K. Wieghardt for the magnetic measurements and Professor K. M. Salikhov for helpful discussions. Support from the Russian Foundation for Basic Research No. 01–03–32270 is greatly appreciated.

<sup>[1]</sup> L. R. Melby, R. J. Herder, W. Mahler, R. E. Benson, W. E. Mochel, *J. Am. Chem. Soc.* **1962**, *84*, 3374.

<sup>[2]</sup> L. Ballester, A. Gutiérrez, M. F. Perpiñán, M. T. Azcondo, *Coord. Chem. Rev.* **1999**, *190–192*, 447.



- [3] [3a] A. H. Reis Jr., L. D. Preston, J. M. Williams, S. W. Peterson, G. A. Candela, L. J. Schwartzendruber, J. S. Miller, *J. Am. Chem. Soc.* **1979**, *101*, 2756. [3b] W. E. Broderick, J. A. Thompson, E. P. Day, B. M. Hoffman, *Science* **1990**, *249*, 401. [3c] W. E. Broderick, B. M. Hoffman, *J. Am. Chem. Soc.* **1991**, *113*, 6334.
- [4] [4a] J. B. Torrance, *Acc. Chem. Res.* **1979**, *12*, 79. [4b] M. T. Azcondo, L. Ballester, E. Coronado, A. M. Gil, C. Gómez, A. Gutiérrez, M. F. Perpiñán, J. Ramos, A. E. Sánchez, *Synth. Met.* **1997**, *86*, 1833. [4c] L. Ballester, A. M. Gil, A. Gutiérrez, M. F. Perpiñán, M. T. Azcondo, A. E. Sánchez, U. Amador, J. Campo, F. Palacio, *Inorg. Chem.* **1997**, *36*, 5291.
- [5] J. S. Miller, A. J. Epstein, *Angew. Chem. Int. Ed. Engl.* **1994**, *33*, 385.
- [6] H. Endres, in J. S. Miller (Ed.), *Extended Linear Chain Compounds*, vol. 3, Plenum, New York, **1983**, p. 263.
- [7] W. Kaim, M. Moscherosch, *Coord. Chem. Rev.* **1994**, *129*, 157.
- [8] P. Kundeler, P. J. Koningsbruggen, J. P. Cornelissen, A. N. van der Host, A. M. van der Kraan, A. L. Spek, J. A. Haasnoot, J. Reedijk, *J. Am. Chem. Soc.* **1996**, *118*, 2190.
- [9] [9a] L. Ballester, M. C. Barral, A. Gutiérrez, A. Monge, M. F. Perpiñán, C. Ruiz Valero, A. Sánchez-Pelaez, *Inorg. Chem.* **1994**, *33*, 2142. [9b] L. Ballester, A. Gutiérrez, M. F. Perpiñán, U. Amador, M. T. Azcondo, A. E. Sánchez, C. Bellitto, *Inorg. Chem.* **1997**, *36*, 6390. [9c] L. Ballester, A. M. Gill, A. Gutiérrez, M. F. Perpiñán, M. T. Azcondo, A. E. Sánchez, E. Coronado, C. J. Gómez-García, *Inorg. Chem.* **2000**, *39*, 2837.
- [10] [10a] J. P. Cornelissen, J. H. van Diemen, L. R. Groeneveld, J. G. Haasnoot, A. L. Spek, J. Reedijk, *Inorg. Chem.* **1992**, *31*, 198. [10b] M. T. Azcondo, L. Ballester, A. Gutiérrez, M. F. Perpiñán, U. Amador, C. Ruiz-Valero, C. Bellitto, *J. Chem. Soc., Dalton Trans.* **1996**, 3015.
- [11] A. M. Madalan, H. W. Roesky, M. Andruh, M. Noltemeyer, N. Stanica, *Chem. Commun.* **2002**, 1638.
- [12] O. Jiménez-Sandoval, D. Ramírez-Rosales, M. del Jesús Rosales-Hoz, M. E. Sosa-Torres, R. Zamorano-Ulloa, *J. Chem. Soc., Dalton Trans.* **1998**, 1551.
- [13] G. M. Sheldrick, SHELXL-97, *Program for Crystal Structure Refinement*, University of Göttingen, Germany, **1997**.
- [14] [14a] O. Kahn, *Molecular Magnetism*, VCH Publishers, New York, **1993**, p. 258. [14b] M. E. Fisher, *Am. J. Phys.* **1964**, *32*, 343.
- [15] P. W. Anderson, P. R. Weiss, *Rev. Mod. Phys.* **1953**, *25*, 269.
- [16] E. Pleau, G. Kokoszka, *J. Chem. Soc., Faraday Trans. 2* **1973**, *69*, 355.
- [17] R. Kubo, K. Tomita, *J. Phys. Soc.* **1954**, *9*, 888.
- [18] Yu. N. Molin, K. M. Salikhov, K. I. Zamaraev, *Spin Exchange Principles and Application in Chemistry and Biology*, Springer, Berlin, **1980**.

Received November 11, 2002